ISSN 0023-1584, Kinetics and Catalysis, 2012, Vol. 53, No. 3, pp. 363–373. © Pleiades Publishing, Ltd., 2012.
Original Russian Text © S.A. Yashnik, V.F. Anufrienko, V.A. Sazonov, Z.R. Ismagilov, V.N. Parmon, 2012, published in Kinetika i Kataliz, 2012, Vol. 53, No. 3, pp. 377–388.

Low-Temperature Activation of Nitrogen Oxide on Cu–ZSM-5 Catalysts

S. A. Yashnik, V. F. Anufrienko, V. A. Sazonov, Z. R. Ismagilov, and V. N. Parmon
Boreskov Institute of Catalysis, Siberian Branch, Russian Academy of Sciences, Novosibirsk, 630090 Russia
e-mail: yashnik@catalysis.ru

Received January 15, 2010

Abstract—The adsorption and activation of NO molecules on Cu–ZSM-5 catalysts with different Cu/Al and Si/Al ratios (from 0.05 to 1.4 and from 17 to 45, respectively) subjected to different pretreatment was studied by ultraviolet-visible diffuse reflectance (UV-Vis DR). It was found that the amount of chemisorbed NO and the catalyst activity in NO decomposition increased with an increase in the Cu/Al ratio to 0.35–0.40. The intensity of absorption bands at 18400 and 25600 cm^{-1} in the UV-Vis DR spectra increased symbatically. It was hypothesized that the adsorption of NO occurs at Cu^+ ions localized in chain copper oxide structures with the formation of mono- and dinitrosyl Cu(I) complexes, and this process is accompanied by the $Cu^{2+}...Cu^+$ intervalence transfer band in the region of 18400 cm^{-1}. The low-temperature activation of NO occurs through the conversion of the dinitrosyl Cu(I) complex into the π-radical anion $(N_2O_2)^-$ stabilized at the Cu^{2+} ion of the chain structure, $[Cu^{2+}–cis\text{-}(N_2O_2)^-]$, by electron transfer from the Cu^+ ion to the *cis* dimer $(NO)_2$. This complex corresponds to the $L \rightarrow M$ charge transfer band in the region of 25600 cm^{-1}. The subsequent destruction of the complex $[Cu^{2+}–cis\text{-}(N_2O_2)^-]$ at temperatures of 150–300°C leads to the release of N_2O and the formation of the complex $[Cu^{2+}O^-]$, which further participates in the formation of the nitrite–nitrate complexes $[Cu^{2+}(NO_2)^-]$, $[Cu^{2+}(NO)(NO_2)^-]$, and $[Cu^{2+}(NO_3)^-]$ and NO decomposition products.

DOI: 10.1134/S0023158412030135

INTRODUCTION

A common opinion concerning the unique catalytic properties of copper-substituted zeolites, especially Cu–ZSM-5, in the decomposition of nitrogen oxides [1–3] and the selective catalytic reduction of NO with C_2–C_4 hydrocarbons [4–8] has been formed in the past two decades. For understanding the nature of the catalytic activity of Cu–ZSM-5, it is important to have information on the electronic structure of copper cations, their coordination, mutual association, and localization in the structure of Cu-substituted ZSM-5 and also on changes in the individual electronic states of copper upon the adsorption of NO, oxygen, and light hydrocarbon molecules.

It was found by various physicochemical techniques that Cu–ZSM-5 contains isolated ions stabilized in cation-exchange sites of the zeolite [1, 7, 8], copper ions coordinated to extra-framework bridging oxygen [7–12], and copper ions bound to extra-framework aluminum cations [13]. The electronic state and geometry of Cu^{2+} cations containing extra-framework oxygen and also their structural transformations in the reaction atmosphere are the most controversial subjects. It is believed that the bridging copper dimers $[Cu–O–Cu]^{2+}$ [7], bis(μ-oxo)-$[Cu_2O_2]$ complexes [9], the square-planar oxide clusters $(Cu_2O_2)_n$ [8, 10, 11], and the chain copper oxide structures $(CuO)_n$ [8, 12] occur in Cu–ZSM-5.

In this work, we used ultraviolet-visible diffuse reflectance (UV-Vis DR) spectroscopy to study the adsorption and activation of NO molecules on Cu–ZSM-5 samples with different electronic states of copper cations depending on NO pressure and temperature.

EXPERIMENTAL

The *a*Cu-ZSM-5-*b*-*c* catalysts, where *a* is the copper content (wt %) and *b* and *c* are the Si/Al and Cu/Al atomic ratios, respectively, were prepared in accordance with a procedure described elsewhere [12]. For this purpose, the ion exchange of H–ZSM-5 zeolite with aqueous (pH ~6) or ammonia (pH ~10) solutions of copper acetate was performed at a solution : zeolite ratio of 10 and copper acetate concentrations from 0.01 to 0.10 mol/L. In the course of the synthesis, H–ZSM-5 with Si/Al atomic ratios of 17, 30, and 45 and iron contents of 0.09, 0.50, and 0.65 wt %, respectively, were used. After the completion of ion exchange, the suspension was filtered and washed with distilled water, and the sediment was dried in air at 100°C and calcined at 500°C for 2 h. According to data obtained by inductively coupled plasma atomic emission spectrometry (ICP AES), the copper content was 0.3–3.0 wt %.

A system equipped with a diffusion pump, a trap cooled with liquid nitrogen, a gas inlet line, manometers, and heating and temperature-control devices was used for the activation of samples and the adsorption of gases. The activated Cu–ZSM-5 sample with a volume of about 2 cm^3 was placed in an optical cell equipped with a vacuum valve; after the measurement of the UV-Vis DR spectrum of the initial sample, it was kept in an atmosphere of oxygen or in a vacuum at 400°C for 1 h, and the released gases were frozen in the trap with liquid nitrogen. Upon the completion of activation, the valve on the cell was closed, and the cell was detached from the vacuum system; the UV-Vis DR spectrum of the activated sample was measured at room temperature. In some cases, the vacuum activation time was increased to 20 h. Previously, we studied Cu–ZSM-5 samples by electron paramagnetic resonance (EPR) spectroscopy [8]; in this case, we measured the spectra of an initial sample and a sample activated in an atmosphere of oxygen or in a vacuum placed in quartz ampoules under conditions analogous to those described above.

Next, the optical cell with the activated Cu–ZSM-5 sample was placed in the above system, and the adsorption of gases was performed. NO was adsorbed from a volume of 0.35 L at room temperature and a pressure of 0.65–2.6 mbar, and O_2 was adsorbed at 25 and 400°C and pressures of 2–15 mbar and 0.1–0.2 bar, respectively. After the adsorption of gases, the UV-Vis DR spectra were measured; then, the sample was heated at temperatures from 100 to 400°C and the UV-Vis DR spectra were recorded again at each particular temperature.

The UV-Vis DR spectra were measured on a Shimadzu UV-2501PC spectrophotometer with an ISR-240 A attachment. In the recording of the spectra, the absorption compensation with respect to $BaSO_4$ in the range of 11000–54000 cm^{-1} was considered, and the spectra were represented as the Kubelka–Munk function $F(R)$ after computer processing.

EPR spectra were measured on a Bruker ER 200D spectrometer with $\lambda = 3$ cm, magnetic field modulation of 100 kHz, and a magnetic field to 5000 G at a temperature of 77 K. The parameters of the EPR spectra were determined by their comparison with the spectrum of diphenylpicrylhydrazyl ($g = 2.0037 \pm 0.0002$).

The activity of Cu–ZSM-5 samples in NO decomposition was determined in a flow reactor at a gas supply space velocity of 5200 h^{-1} in the temperature range of 150–450°C. The reaction mixture contained 1.5 vol % NO in argon. The catalyst (grain size of 1–2 mm) was mixed with quartz (particle size of 1–2 mm) in a ratio of 1 : 1. The catalyst volume was 1 cm^3. The reaction mixture and reaction products were analyzed on an ECOM-SG^{plus} gas analyzer (the accuracy of the determination of NO and NO_2 was 1 ppm, and the accuracy of the determination of O_2 was 0.1 vol %) and on a Kristall 2000M gas chromatograph with a thermal conductivity detector. A packed column with the Porapak Q phase was used for the determination of N_2O, and a column with molecular sieves 5 Å was used for the separation of N_2, O_2, and NO. The carrier-gas (helium) flow rate was 30 mL/min, and the column temperature was 90°C. The activity of the catalyst was characterized by the rate of NO conversion (w_{NO}, μmol $(g_{cat})^{-1}$ min^{-1}) at a specified temperature, which was calculated on the assumption that the reactor is a plug-flow reactor and the reaction is of first order with respect to NO. The selectivity of the catalyst was evaluated according to the degrees of conversion of NO into N_2, NO_2, and N_2O.

RESULTS AND DISCUSSION

Electronic State and Redox Properties of Copper Cations

Earlier [8], we studied the electronic state of copper cations in the Cu–ZSM-5 catalysts, which were used in this work. The following three types of the stabilization of copper cations in Cu–ZSM-5 with different copper contents and different Si/Al atomic ratios were detected by EPR spectroscopy and UV-Vis DR: (1) isolated Cu^{2+} ions stabilized in the cation-exchange sites of the zeolite, (2) chain copper oxide structures in zeolite channels, and (3) square-planar oxide clusters localized on the external surface of crystallites. The relative concentration of copper ions stabilized in the specified states in the ion-exchange Cu–ZSM-5 samples, depended on the catalyst preparation method and Cu/Al and Si/Al atomic ratios [8]. For example, it was shown that isolated Cu^{2+} ions were predominant in the samples with low Cu/Al and Si/Al ratios, whereas the square-planar oxide clusters of copper predominated in the samples with a Cu/Al ratio above 0.5 prepared from ammonia solutions with pH 10. The electronic state and localization of copper ions are responsible for the redox properties of Cu–ZSM-5 and the accessibility of copper centers to the adsorption of different molecules. The electronic state of copper cations and their redox properties characteristic of each type of stabilization are briefly considered below.

The isolated ions of Cu^{2+} in the initial Cu–ZSM-5 samples (before activation) manifested themselves as an anisotropic signal with the parameters $g_{\parallel} = 2.38$, $A_{\parallel} = 135$ G, and $g_{\perp} = 2.08$ in the EPR spectrum (type A, curve *1* in Fig. 1) and as the *d–d* transition and the $O^{2-} \rightarrow Cu^{2+}$ charge transfer (CT) band in the regions of 12200–12500 and 46500–48000 cm^{-1}, respectively, in UV-Vis DR (Fig. 2, curve *1*) [8]. The above parameters of the EPR spectrum and the energies of absorption bands (the *d–d* transition and the L → M CT band) are characteristic of Cu^{2+} ions with the $d_{x^2-y^2}$ ground state in an octahedral coordination (Cu^{2+}_{Oh}), which are similar to the hexaaqua complex $[Cu(H_2O)_6]^{2+}$ [14]. The activation of Cu–ZSM-5 samples in a vacuum or in oxygen at 400°C, which caused their dehydration, was accompanied by a decrease in the intensity of the EPR signal of isolated Cu^{2+} ions and by a change in their parameters to the values of $g_{||} = 2.28–2.33$ and $A_{||} = 142–164$ G (types B and C, curve *2* in Fig. 1). In the UV-Vis DR spectra of the activated Cu–ZSM-5 samples, a wide absorption band at 12500–14500 cm^{-1} was observed (Fig. 2, curve *2*). Changes in the EPR and UV-Vis DR spectra of the activated samples are indicative of a tetragonal distortion (extension) of the octahedral field of ligands in the coordination sphere of isolated Cu^{2+}_{Oh} ions [14], which can be caused by the partial removal of H_2O ligands. In this case, the broadening of a band at 12500–14500 cm^{-1} is a consequence of the splitting of electronic bands due to the *d–d* transitions of isolated Cu^{2+} ions in fields with the tetragonal symmetry (for example, with a square-planar coordination). A characteristic property of the isolated Cu^{2+} ions in Cu–ZSM-5 is their two-step reduction initially to Cu^+ and then to Cu^0; the second step occurs at a sufficiently high temperature of about 400°C [15, 16].

The square-planar oxide clusters of copper $(Cu_2O_2)_n$, which mainly occur on the outer surface of zeolite crystallites, are characterized by the $O^{2-} \to Cu^{2+}$ CT band in the region of 30000–32000 cm^{-1} in the UV-Vis DR spectra. Usually, they are observed in the ion-exchange Cu–ZSM-5 catalysts after their activation in a vacuum or in an atmosphere of oxygen [8]. The low energy of the $O^{2-} \to Cu^{2+}$ CT band is indicative of the high covalency of the Cu–O bond in these structures, which is consistent with the results of the temperature-programmed reduction of Cu–ZSM-5 with hydrogen and by carbon monoxide [10, 15]. These structures are more easily reduced to Cu^0 than isolated Cu^{2+} ions; in this case, the reduction at temperatures to 200°C occurs in one step analogously to the reduction of highly dispersed copper oxide [10, 15].

Among the electronic states of copper in Cu–ZSM-5, copper ions bound to extra-framework oxygen and localized in zeolite channels are of the greatest interest. They can be represented as bis(μ-oxo)-$[Cu_2O_2]$ complexes [9] and $Cu^{2+}–O^{2-}–Cu^{2+}–O^{2-}$ chain structures [8, 12], in which the adjacent Cu^{2+} ions are bound to each other by two or one bridging oxygen. The copper dimer $[Cu–O–Cu]^{2+}$ is a special case of chain structures [7]. Under mild conditions, the reversible ion reduction $Cu^{2+} \leftrightarrow Cu^+$ [17] (rather than Cu^0) and the stabilization of the mixed-valence bound states $Cu^{2+}...Cu^+$ were observed in these structures [12]. The capability of the structures containing Cu^{2+} ions and extra-framework oxygen for reversible reduction can play an important role in the adsorption and conversion of molecules in a number of oxidation–reduction reactions.

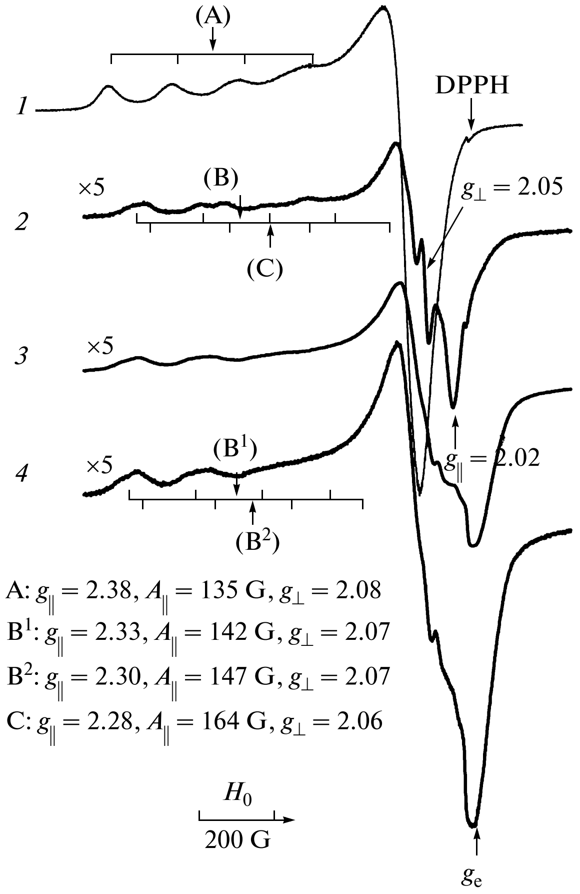

Fig. 1. EPR spectra of (*1*) the initial sample 3.4Cu–ZSM-5–45–1.37 and the sample successively subjected to (*2*) vacuum activation at 400°C for 1 h and the adsorption of water vapor at 25°C and pressures of (*3*) 9 and (*4*) 22 mbar. The parameters of the EPR spectra of isolated ions of the types A, B^1, B^2, and C are specified.

The redox properties of chain structures, which manifest themselves in the internal (physical) reduction–oxidation process $Cu^{2+} + O^{2-}(d^9, p^6) \leftrightarrow Cu^+ + O^-(d^{10}, p^5)$ are caused by their electronic structure, and they depend on the degree of hydration of the system. Thus, according to quantum-chemical calculations [18, 19], the 3*d* levels of Cu^{2+} in linear (quasi-linear) structures with the formal oxidation number 2+, for example, in the molecules of $Cu(OH)_2$ and CuO [18], are close in energy to the *p* level of oxygen. As a result of this, the level with the preferred electron localization on the *p* orbitals of oxygen, which formally corresponds to the state $[Cu^+O^-]$ with the (d^{10}, p^5) electron configuration, becomes partially occupied. At the same time, the adsorption of two water molecules, in particular, on the molecule of $Cu(OH)_2$ [18], leads to the oxidation of Cu(I), and a state of the system that corresponds to $[Cu^{2+}O^{2-}]$ with an unpaired electron on the *d* orbital of copper (d^9, p^6) becomes the ground state. Analogous effects of the electron density redis-

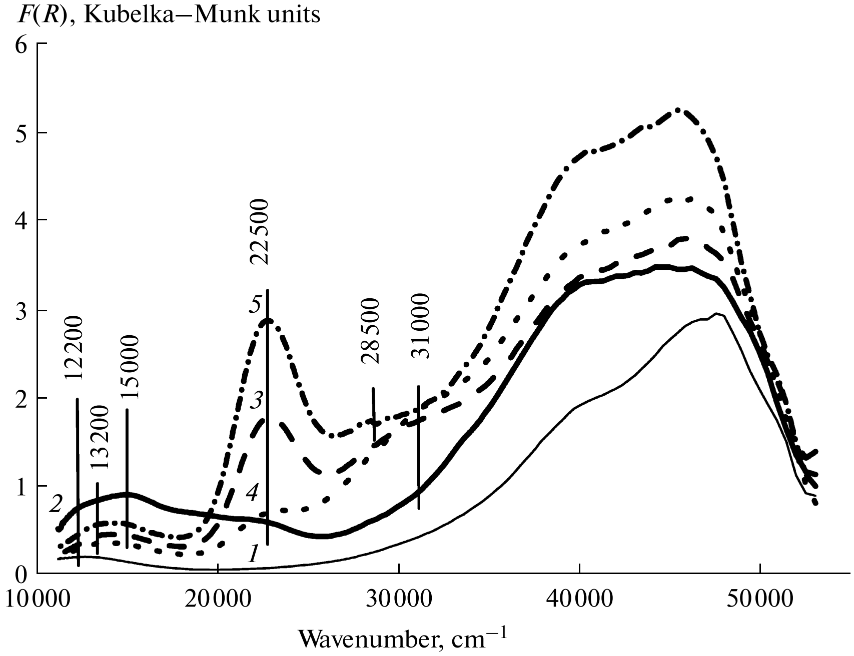

Fig. 2. UV-Vis DR spectra of (*1*) the initial sample 2.7Cu–ZSM-5–17–0.57 and the sample successively subjected to (*2*) vacuum activation at 400°C for 20 h, (*3*) the adsorption of O_2 at 400°C and a pressure of 0.1 bar, (*4*) evacuation at 400°C for 0.5 h, and (*5*) the adsorption of O_2 at 400°C and a pressure of 0.2 bar.

tribution of an unpaired electron are characteristic of the model chain structure O^{2-}–Cu^{2+}–O^{2-}–Cu^{2+} localized on the Al^{3+} ion of the zeolite matrix upon the adsorption and desorption of four water molecules [19]. In the EPR spectra of Cu–ZSM-5 samples, the redistribution of electron density on the Cu^{2+} ions manifests itself as signals due to the O^- radical anion ($g_\perp = 2.05$, $g_\parallel = 2.02$) and Cu^{2+} ions with the d_{z^2} ground state ($g = g_e$ without hyperfine structure splitting), which are observed against the background of isolated Cu^{2+} ions (types B and C) upon dehydration (Fig. 1, curve *2*) and hydration (types B^1 and B^2, curves *3* and *4* in Fig. 1, respectively). These EPR signals are indicative of the stabilization of reduced ($[Cu^+O^-]$) and oxidized ($[Cu^{2+}O^{2-}]$) chain copper oxide structures in zeolite channels [8]. In the UV-Vis DR spectra of Cu–ZSM-5, the effects of electron density redistribution on the Cu^{2+} ions of chain structures appear after dehydration at 400°C in a vacuum (Fig. 3a, curve *1*) or in oxygen (Fig. 3b, curve *1*) in the form of the intervalent transition (IVT) $Cu^{2+}\ldots Cu^+$ at 22 500 cm^{-1}. These signals disappear after hydration [8].

The redox properties of chain copper oxide structures in the channels of Cu–ZSM-5 zeolite manifest themselves in chemical reduction and oxidation upon the adsorption and activation of NO and O_2 molecules with the participation of which the decomposition of NO and the selective reduction of NO by hydrocarbons occur.

Electronic State of Copper Cations upon the Adsorption of Oxygen

As noted above, according to UV-Vis DR data, the samples of Cu–ZSM-5 with Cu/Al ≥ 0.5 after activation (dehydration) in an atmosphere of oxygen or in a vacuum at 400°C for 1 h (curves *1* in Figs. 3a and 3b) and 20 h (Fig. 2, curve *2*) contained isolated Cu^{2+} ions (12000–14500 cm^{-1}), chain copper structures in a mixed-valence state ($Cu^{2+}\ldots Cu^+$ intervalent transition band at 22500 cm^{-1}), and square-planar copper oxide clusters ($O^{2-} \rightarrow Cu^{2+}$ CT band at 30000–32000 cm^{-1}). Using the sample 2.7Cu–ZSM-5–17–0.57 as an example (Figs. 2 and 3), let us consider how the electronic states of different copper ions change upon the adsorption of oxygen and NO.

The adsorption of small oxygen amounts (28.5 μmol at a pressure of 2 mbar and a temperature of 25°C) on Cu–ZSM-5 does not lead to a change in the UV-Vis DR and EPR spectra. In the EPR spectra, the signals of isolated Cu^{2+} ions with different degrees of the tetragonal distortion of an octahedron ($g'_\parallel$ = 2.30–2.33, $A'_\parallel$ = 145–150 G, and $g'_\perp$ = 2.06–2.07; $g''_\parallel$ = 2.28, $A''_\parallel$ = 165 G, and $g''_\perp$ = 2.06) and the signal of the O^- radical anion ($g_\parallel = 2.02$, $g_\perp = 2.05$) were present. The parameters and intensities of these signals are characteristic of the Cu–ZSM-5 samples activated in a vacuum (Fig. 1, curve *2*). As the amount of adsorbed oxygen was increased to 150 μmol (10 mbar), the intensity of the EPR signals of isolated Cu^{2+} ions decreased; in this case, the intensity of a signal from Cu^{2+} ions with a strong tetragonal distortion ($g_{\|}'' = 2.28$) decreased to a greater degree. A further increase in the amount of adsorbed oxygen to 1.5–3.0 mmol (0.1–0.2 bar) led to the dipole–dipole broadening of the EPR spectrum; as a result of this, the signal intensity of the isolated Cu^{2+} ions considerably decreased so that it becomes difficult to estimate a change in their concentration.

The adsorption of oxygen at 400°C and a pressure of 0.1–0.2 bar on the sample 2.7Cu–ZSM-5–17–0.57 activated in a vacuum caused a reversible increase in the intensity of the $Cu^{2+}...Cu^{+}$ IVT band (22500 cm^{-1}) and the $O^{2-} \rightarrow Cu^{2+}$ CT band of square-planar copper oxide clusters (28000–32000 cm^{-1}, curves *3* and *5* in Fig. 2). The removal of oxygen from the gas phase at 400°C first led to a decrease in the intensity of the $Cu^{2+}...Cu^{+}$ IVT band (Fig. 2, curve *4*). In both cases, the absorption band intensity at 13700 cm^{-1}, which corresponds to the *d–d* transitions of isolated Cu^{2+} ions, remained almost unchanged (Fig. 2, curves *3–5*). It is believed that, in the course of vacuum activation, the internal reduction of the Cu^{2+} ions of chain structures to Cu^{+} (d^{10}, $S = 0$), which do not give an EPR signal and absorption bands in the visible region of UV-Vis DR, occurs. It is likely that oxygen is adsorbed on the closely spaced $Cu^{+}...Cu^{+}$ ions of chain structures in zeolite channels. The oxidation of one of them is accompanied by the formation of the $Cu^{2+}...Cu^{+}$ mixed-valence pairs (IVT band at 22500 cm^{-1}). Upon the oxidation of both Cu^{+} ions, centers similar to the square-planar oxide dimer of copper in electronic structure (L → M CT band, 32000 cm^{-1}) are formed in zeolite channels.

Electronic State of Copper Cations upon the Adsorption of Nitrogen Oxide

Because we used H–ZSM-5 zeolites containing from 0.1 to 0.6 wt % iron impurities for the preparation of Cu–ZSM-5, we initially performed experiments with the unmodified initial samples of H–ZSM-5 in order to evaluate the role of Fe^{3+} cations in the adsorption of NO. Upon the adsorption of NO on them (at pressures of 2.5 and 25.0 mbar), the UV-Vis DR spectra exhibited three absorption bands (at 15500, 24300, and 27200 cm^{-1}), whose intensity was lower by an order of magnitude than the intensity of bands in this region upon the adsorption of NO on Cu–ZSM-5. Furthermore, the intensity did not depend on the Fe content of H–ZSM-5 and on the pressure of NO.

The spectrum of gaseous NO added to an evacuated empty cell (with no sample) is characterized by low-intensity absorption in the region of 42000–45000 cm^{-1}, whereas absorption bands are completely absent from the region of 11000–40000 cm^{-1}; this is consistent with published data [22]. In the spectrum of gaseous NO_2, which can be formed upon the oxidation of NO in the presence of the Cu–ZSM-5 catalyst in the course of the consecutive reactions $2NO \rightarrow N_2 + O_2$ and $2NO + O_2 \rightarrow 2NO_2$ [7, 20] or the disproportionation $3NO \rightarrow N_2O + NO_2$ [21], there are low-intensity absorption bands at 24300 and 29200 cm^{-1} and an intense band in the UV region at 50100 cm^{-1}, which correspond to n*–π*, π*–σ*, and π–π* transitions, respectively [14, 22]. The low intensity of absorption bands in the region of 15000–35000 cm^{-1}, which are characteristic of H–ZSM-5 and gaseous NO_2, and the absence of these bands from the spectrum of gaseous NO allow us to attribute absorption bands in the UV-Vis DR spectra upon the adsorption

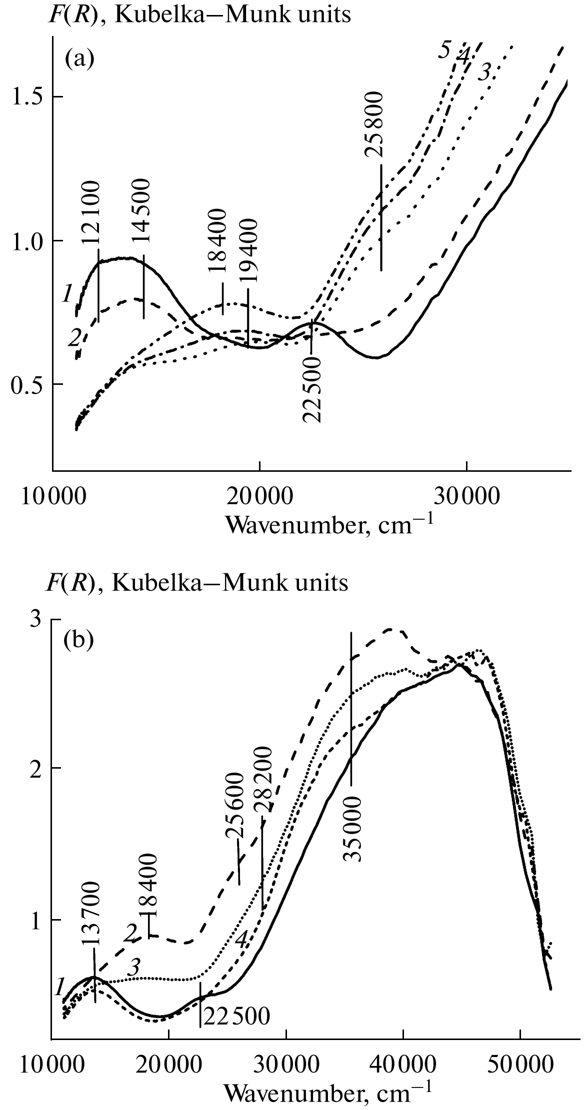

Fig. 3. UV-Vis DR spectra of the sample 2.7Cu–ZSM-5–17–0.57 after the following treatment: (a) (*1*) vacuum activation at 400°C for 1 h; NO adsorption at 25°C and pressures of (*2*) 0.65, (*3*) 2, (*4*) 6.5, and (*5*) 13 mbar; (b) (*1*) activation in an atmosphere of oxygen at 400°C for 1 h; (*2*) NO adsorption at 25°C and a pressure of 25 mbar; and thermal treatment for 0.5 h at (*3*) 150 and (*4*) 300°C.

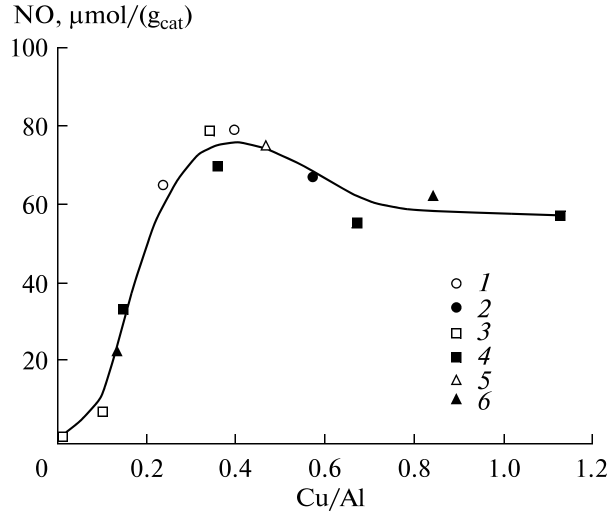

Fig. 4. Dependence of the amount of NO chemisorbed on Cu–ZSM-5 samples at 25°C and an initial pressure of 2.6 mbar upon the Cu/Al atomic ratio. The samples were synthesized on H–ZSM-5 zeolite with Si/Al of (*1*, *2*) 17, (*3*, *4*) 30, and (*5*, *6*) 45 from the solutions of copper acetate with pH (*1*, *3*, *5*) ~6 and (*2*, *4*, *6*) ~10.

of NO on Cu–ZSM-5 to copper ions and a change in their electronic state and coordination environment.

The adsorption of small NO amounts (9.5 μmol at a pressure of 0.65 mbar and a temperature of 25°C) in the activated sample 2.7Cu–ZSM-5–17–0.57 does not influence its electronic spectrum (Fig. 3a, curve *1*) in the region of the *d–d* transition of the isolated Cu^{2+} ions (12100–14500 cm^{-1}), but it leads to noticeable changes in the $Cu^{2+}\ldots Cu^{+}$ IVT region (18400–22500 cm^{-1}, curve *2* in Fig. 3a). As the pressure of NO was increased to 6.5–25.0 mbar (95–380 μmol), the intensity of the *d–d* transition of isolated Cu^{2+} ions (13800 cm^{-1}) remained almost unchanged, whereas the $Cu^{2+}\ldots Cu^{+}$ IVT band intensity (18400 cm^{-1}) gradually increased. Furthermore, as the pressure of NO was increased, the L → M CT band (25600 cm^{-1}) of the dimers of copper exchange-bound through bridging oxygen appeared in the spectrum (Fig. 3a, curves *3*–*5*).

Analogous changes in the electronic spectra of Cu–ZSM-5, namely, the appearance of the $Cu^{2+}\ldots Cu^{+}$ IVT band (18400 cm^{-1}) and the L → M CT band of the dimers of copper (25600 cm^{-1}), were also observed upon the adsorption of NO (Fig. 3b, curve *2*) on the Cu–ZSM-5 samples activated in oxygen (Fig. 3b, curve *1*). The experimental results clearly indicate that the intensity of the absorption band at 13700 cm^{-1}, which corresponds to the *d–d* transition of isolated Cu^{2+}_{Oh} ions in a tetragonally distorted octahedral coordination, remained unchanged after the adsorption of NO on the activated sample. Note that the intensities of the $Cu^{2+}\ldots Cu^{+}$ IVT band (18400 cm^{-1}) and the amounts of NO chemisorbed on the samples activated both in a vacuum and in oxygen practically coincide at the same pressure of NO. For example, the amount of NO chemisorbed on the sample 2.0Cu–ZSM-5–17–0.40 activated either in a vacuum or in oxygen at 400°C was 57 μmol per gram of the catalyst.

Summarizing the results of studying the adsorption of NO on Cu–ZSM-5 at a temperature of 25°C, we can make a number of conclusions and assumptions that follow from UV-Vis DR data. First, the similar intensities of the *d–d* transitions of isolated Cu^{2+} ions in the tetragonally distorted octahedral coordination sphere before and after the adsorption of nitrogen oxide indicate that these ions, which are characterized by a band at 12100–14500 cm^{-1} in the UV-Vis DR spectra, do not change their coordination state after the adsorption of NO. It is likely that their amount also remained unchanged. Second, the appearance of the $Cu^{2+}\ldots Cu^{+}$ IVT band and the L → M CT band of the dimers of copper suggests the participation of closely spaced Cu^{+} and/or Cu^{2+} copper ions, which, for example, enter into the composition of chain structures containing no less than two copper ions. These centers occur in the Cu–ZSM-5 samples activated both in a vacuum and in oxygen. Third, in the spectra of the Cu–ZSM-5 samples with copper contents from 0.3 to 3 wt %, an absorption band at 25600 cm^{-1} appears only after the addition of NO in an amount close to or larger than that is required for chemisorption. The absorption band intensity at 25600 cm^{-1} and the amount of chemisorbed NO (Fig. 4) increase as the Cu/Al atomic ratio is increased from 0 to 0.35–0.40; then, it remains almost unchanged over the range of Cu/Al ratios from 0.40 to 0.50. As the Cu/Al ratio is further increased, there is a weak tendency toward a decrease in the amount of chemisorbed NO, whereas the intensity of a band at 25600 cm^{-1} remains almost unchanged. Note that the molar ratios of the amount of chemisorbed NO to the total amount of copper in Cu–ZSM-5 in all of the test samples were lower than 1. For example, they were 0.08, 0.27, and 0.16 in the samples 0.3Cu–ZSM-5–30–0.1, 1.1Cu–ZSM-5–30–0.35, and 1.7Cu–ZSM-5–30–0.50, respectively. The low NO/Cu ratios indicate that copper does not entirely participate in the chemical adsorption of NO; in this case, the fraction of "active copper" reaches a maximum in the samples with Cu/Al = 0.25–0.45. Fourth, the low energy of the $O^{2-} \to Cu^{2+}$ CT band of the dimer of copper at 25600 cm^{-1} observed upon the adsorption of NO is indicative of a higher covalency of the Cu–O bond, as compared with the well-known dimer $[Cu^{2+}–O^{2-}–Cu^{2+}]^{2+}$ (L → M CT band at 27000 cm^{-1} [14]), and the presence of a bidentate ligand in the coordination sphere of the Cu^{2+} ion. Fifth, after the adsorption of NO, the Cu–ZSM-5 samples change their color from blue to reddish.

Analyzing the changes in the UV-Vis DR spectra of Cu–ZSM-5 after the adsorption of NO at room temperature, we assumed that the adsorption of NO occurs at the closely spaced Cu^{+} ions of chain structures with the initial formation of the mono- and dinitrosyl complexes of copper(I) $[\mathrm{Cu}^{2+}\cdots\mathrm{Cu}^{+}\text{–}(\mathrm{NO})]$ and $[\mathrm{Cu}^{2+}\cdots\mathrm{Cu}^{+}\text{–}(\mathrm{NO})_2]$, respectively. The rearrangement of two nitrosyl ligands adsorbed at the Cu^{+} ion into the *cis* dimer $\mathrm{N_2O_2}$ leads to the formation of the complex $[\mathrm{Cu}^{2+}\cdots\mathrm{Cu}^{+}\text{–}cis\text{-}(\mathrm{N_2O_2})]$ with the bidentate ligand and then to the activation of NO as a result of electron transfer form the *d* orbital of the Cu^{+} ion to the binding molecular π orbital of the *cis* dimer $\mathrm{N_2O_2}$ [19]. Formally, this process corresponds to the formation of the π-radical anion $(\mathrm{N_2O_2})^-$ stabilized at the Cu^{2+} ion. According to the data of quantum-chemical calculations [19], the *cis* dimer $\mathrm{N_2O_2}$ possesses high electron affinity ($E_\mathrm{a} = -1.3$ eV); therefore, in the case of its stabilization at the electron-donor center of Cu^{+}, the formation of $[\mathrm{Cu}^{2+}\text{–}cis\text{-}(\mathrm{N_2O_2})^-]$ can occur as a result of the oxidation of Cu^{+} with electron transfer to the *cis* dimer $\mathrm{N_2O_2}$. According to published data [23], the dinitrosyl complex $\mathrm{NO\text{–}Cu^{+}\text{–}ON}$ with a cyclic structure is formed without an activation barrier from a mononitrosyl complex in the case of the addition of NO to Cu^{+} through oxygen. In contrast to the weakly bound molecular *cis* dimer (2.23 Å [24]), the π-radical anion $(\mathrm{ONNO})^-$ is characterized by a short length of the N–N bond (1.3–1.4 Å [19, 23, 25]), which also ensures its subsequent disintegration mainly into $\mathrm{N_2O}$ and the $[\mathrm{Cu}^{2+}\text{–}\mathrm{O}^-]$ center [19] or F center [26]. This disintegration occurs at a noticeable rate even at room temperature [23, 26]. Quantum-chemical calculations also showed that the formation of the $[\mathrm{Cu}^{2+}\text{–}cis\text{-}(\mathrm{N_2O_2})^-]$ center is energetically more favorable for the Cu^{+} ions localized in chain structures containing two or more copper ions than at the isolated ions of copper [19]. In this case, it is likely that the role of the second closely spaced copper cation consists in the formation of a “buffer system” because redox properties in $\mathrm{Cu}^{2+}\text{–(O)–}\mathrm{Cu}^{+}$ pairs occur more easily due to the possibility of an internal redistribution of electron density. Thus, the adsorption and activation of NO on Cu–ZSM-5 can be represented as follows:

$$[\mathrm{Cu}^{2+}\cdots\mathrm{Cu}^{+}] + \mathrm{NO} \leftrightarrow [\mathrm{Cu}^{2+}\cdots\mathrm{Cu}^{+}\text{–}(\mathrm{NO})] + \mathrm{NO} \leftrightarrow [\mathrm{Cu}^{2+}\cdots\mathrm{Cu}^{+}\text{–}(\mathrm{NO})_2]$$
$$\leftrightarrow [\mathrm{Cu}^{2+}\cdots\mathrm{Cu}^{+}\text{–}cis\text{-}(\mathrm{N_2O_2})],$$

$$[\mathrm{Cu}^{2+}\cdots\mathrm{Cu}^{+}\text{–}cis\text{-}(\mathrm{N_2O_2})](\mathrm{Cu}^{2+}\ldots\mathrm{Cu}^{+}\ \text{IVT band})$$
$$\leftrightarrow [\mathrm{Cu}^{2+}\cdots\mathrm{Cu}^{2+}\text{–}cis\text{-}(\mathrm{N_2O_2})^-](\mathrm{O}^{2-} \to \mathrm{Cu}^{2+}\ \text{CT band}).$$

For evaluating the stability of the complex $[\mathrm{Cu}^{2+}\text{–}cis\text{-}(\mathrm{N_2O_2})^-]$, we performed two series of experiments on the thermal treatment of Cu–ZSM-5 samples at 50–400°C after the adsorption of NO. In the first series, were initially removed NO from a gas phase by evacuation at room temperature for 1 h. After the removal of NO, a decrease in the intensity of the $\mathrm{Cu}^{2+}\ldots\mathrm{Cu}^{+}$ IVT band in the region of 18400 cm^{-1} was observed in the electronic spectra, whereas the intensity of a band at 25600 cm^{-1} did not change. The latter fact suggests the formation of a stable adsorbed complex with NO on the surface of Cu–ZSM-5. This complex occurs on the sample surface up to a temperature of 150°C, although its concentration decreases as the treatment temperature is increased from room temperature to 150°C; this is evident from a decrease in the intensity of an absorption band at 25600 cm^{-1}. A further increase in the treatment temperature to 300 and 400°C leads to the disappearance of the band at 25600 cm^{-1}, which is indicative of the degradation of the complex. Note that the reddish color intensity of the sample gradually decreases as the treatment temperature of Cu–ZSM-5 is increased from room temperature to 150°C. After treatment at 300°C, the reddish color completely disappears, and the sample becomes blue; this color change is accompanied by the appearance of absorption bands at 12500–13700 cm^{-1} in the UV-Vis DR spectrum. Upon the subsequent vacuum activation of the Cu–ZSM-5 sample at 400°C, absorption bands corresponding to the *d*–*d* transition of isolated Cu^{2+} ions (13000–14000 cm^{-1}) and the $\mathrm{Cu}^{2+}\ldots\mathrm{Cu}^{+}$ IVT band (22500 cm^{-1}) appear, and this fact indicates the reduction of the initial electronic state of the catalyst.

In the second series, the thermal treatment of Cu–ZSM-5 was performed without the removal of NO from the gas phase. In the course of these experiments, it was shown that the thermal treatment of Cu–ZSM-5 at 150°C (Fig. 3b, curve *3*) leads to a decrease in the intensities of the $\mathrm{Cu}^{2+}\ldots\mathrm{Cu}^{+}$ IVT band (18400 cm^{-1}) and the L → M CT band of the dimer of copper (25600 cm^{-1}). In this case, the intensity of the absorption band at 25600 cm^{-1} depends on the pressure of NO in the gas phase and on the time of thermal treatment. For example, the absorption band intensity at 25600 cm^{-1} in the spectrum of the sample 2.7Cu–ZSM-5–17–0.57 after treatment at 150°C for 0.5 h at an NO pressure of 25 mbar in the gas phase was higher than that at pressures of 2 and 6.5 mbar, and it decreased with treatment time. As the treatment temperature was increased to 300°C at a treatment duration of 0.5 h (Fig. 3b, curve *4*), the *d*–*d* transition of isolated Cu^{2+} ions (13800 cm^{-1}) and a shift of the L → M CT band of the dimer of copper from 25600 to 28200–

30000 cm^{-1} were observed in the UV-Vis DR spectrum. This is indicative of the degradation of the adsorbed complex $[Cu^{2+}...Cu^{2+}–cis\text{-}(N_2O_2)^-]$ and the formation of the square-planar complexes of copper.

We also performed an experiment on the adsorption of oxygen at pressures of 2.6 and 13 mbar on the sample 2.7Cu–ZSM-5–17–0.57, which contained adsorbed NO in an amount of 60 μmol/(g_{cat}) (1.7 mbar). The adsorption of oxygen even at 25°C led to the disappearance of the L → M CT band in the region of 25600 cm^{-1}. In our opinion, this is indirect evidence for the formation of an adsorbed dimer of nitrogen(II) oxide on the surface of Cu–ZSM-5 because it is well known that N_2O_2 rather than NO reacts with oxygen in the gas-phase oxidation of NO [27]. In this case, the gas-phase oxidation of NO to NO_2 occurs at a sufficient rate already at room temperature, and the reaction rate dramatically decreases (by a factor of 7000) as the temperature is increased even to 100°C [27].

Thus, the study of the effect of thermal treatment on the electronic state of copper in the Cu–ZSM-5 sample with adsorbed NO showed that the complex $[Cu^{2+}\cdots Cu^{2+}–cis\text{-}(N_2O_2)^-]$ is stable at room temperature, and its degradation comes into play at 150°C and depends on the pressure of NO in the gas phase. According to quantum-chemical calculations [19], N_2O, which is released into the gas phase as a reaction product, and the center $[Cu^{2+}O^-]$ are predominantly formed upon the decomposition of this complex. The complex $[Cu^{2+}\cdots Cu^{2+}–cis\text{-}(N_2O_2)^-]$ easily interacts with molecular oxygen to give NO_2 and Cu^+ as products. At 200–350°C, the center $[Cu^{2+}O^-]$ interacts with NO from the gas phase to be converted into nitrite–nitrate complexes, as reliably demonstrated by IR spectroscopy [28–34]. A comparison with published data shows that the adsorbed nitrite–nitrate complexes can be desorbed from the surface at 400°C without decomposition (in the form of NO_2) [20, 30] and with decomposition to NO and O_2 [31, 32] or N_2 and O_2 [33] at 450°C. The decomposition of the nitrite ($[Cu^{2+}(NO_2)^-]$) and nitrate ($[Cu^{2+}(NO_3)^-]$) complexes is accompanied by the regeneration of Cu^+ and $[Cu^{2+}O^-]$ centers, respectively [29]. As a result of the decomposition of the complex $[Cu^{2+}(NO)(NO_2)^-]$, N_2O is released and the center $Cu^{2+}O_2^-$ is formed [28], which is necessary for the formation of a nitrate complex and oxygen as a product of the direct decomposition of NO [29]. Spoto et al. [33] proposed a similar reaction scheme for the conversion of NO based on IR spectroscopic data; this reaction scheme is based on the assumption of the direct decomposition of the dinitrosyl complex of copper(I) to N_2O with the simultaneous formation of the center $[Cu^{2+}O^-(NO)]$, which subsequently participates in the decomposition of NO through the formation of the $[Cu^{2+}(NO_2)^-(NO)]$ and $[Cu^{2+}O^-]$ complexes. Iwamoto et al. [34] proposed a reaction scheme in which the mono- and dinitrosyl complexes $[Cu^+(NO)^{\delta-}]$ and $[Cu^+(NO)_2^{\delta-}]$ were responsible for the decomposition of NO to N_2O and N_2 at room temperature. In this case, N_2O and N_2 resulted from an intermolecular reaction involving two adjacent copper ions, which interacted with adsorbed $NO^{\delta-}$ and $(NO)_2^{\delta-}$, rather than the dinitrosyl complex $[Cu^+(NO)_2^{\delta-}]$. Note that this reaction scheme cannot explain the formation of N_2 (to 0.46 mole per mole of Cu), which was observed by Iwamoto et al. [34] at room temperature. In our opinion, the adsorption of NO can occur at isolated copper ions; however, for the decomposition of the dinitrosyl complex of copper(I) to N_2O, it should be initially converted into the *cis* dimer N_2O_2 adsorbed at the Cu^+ ion. In this case, the second closely spaced Cu^{n+} cation participates in the redistribution of electron density, and it is necessary for the stabilization of the complex $[Cu^{2+}\cdots Cu^{2+}–cis\text{-}(N_2O_2)^-]$.

Correlation of NO Chemisorption Data for the Cu–ZSM-5 Samples with Their Catalytic Activity in NO Decomposition

The main products of the direct decomposition of NO on the Cu–ZSM-5 catalysts in the range of 150–450°C are N_2 and O_2; however, at temperatures lower than 350°C, N_2O and NO_2 were also present among the reaction products in an amount to 300–400 ppm. Figure 5 shows the temperature dependence of the NO conversion into N_2, N_2O, and NO_2 over the catalyst 1.5Cu–ZSM-5–30–0.44. As can be seen, the total conversion of NO increases with temperature to reach a maximum value (of about 47%) at 350°C (Fig. 5, curve *1*) and then decreases. In this case, the maximum amounts of N_2, N_2O, and NO_2 are formed at temperatures of 400, 250, and 300°C, respectively, whereas N_2O and NO_2 are absent from the reaction products at 450°C.

According to published data [21], the cause of the formation of N_2O and NO_2 below 300°C is the disproportionation of NO ($3NO = N_2O + NO_2$). The formation of NO_2 in the range of 300–350°C can also be due to the interaction of unreacted NO with oxygen [20, 21], which was formed as a result of the direct decomposition of NO ($2NO = N_2 + O_2$ and $NO + 1/2O_2 = NO_2$).

Note that the decomposition of nitrous oxide to nitrogen and oxygen ($N_2O = N_2 + 1/2O_2$) in the presence of Cu–ZSM-5 occurs effectively at temperatures of 300–400°C [3, 35], which can lead to a decrease in the yield of N_2O in the reaction of the direct decomposition of NO at temperatures higher than 300°C. As found previously [20, 21], the decrease in the NO conversion at high temperatures it is caused by a decrease in the contribution of the equilibrium-controlled reaction of NO oxidation to NO_2, whose rate decreases with temperature [27], rather than by catalyst deactivation. Thus, the character of the observed temperature dependence of the NO conversion into N_2, N_2O, and NO_2 on the sample 1.5Cu–ZSM-5–30–0.44 is consistent with published data [20, 21], although the temperature at which a maximum conversion of NO was reached in the cited works was somewhat higher, namely, 400–450°C [20] or 450°C [21]. The difference in temperatures at which Cu–ZSM-5 reached maximum activity in NO decomposition can be due to both different catalyst compositions and different testing conditions, in particular, different concentrations of NO in the reaction mixture and different contact times.

Similar temperature dependences of the NO conversion into N_2, N_2O, and NO_2 were obtained on the other Cu–ZSM-5 test catalysts with copper contents of 0.3–3 wt %; however, the NO conversion and the temperature of a maximum activity depended on the copper content of the catalyst. Thus, on over-exchanged catalysts, the maximum NO conversion was somewhat lower and it was reached at a temperature of about 400°C. For example, on the catalyst 2.8Cu–ZSM-5–30–0.83, the conversion of NO was 38% at 350°C or 39% at 400°C. Figure 6 shows the dependence of the rate of NO decomposition on the Cu/Al ratio at a space velocity of 5200 h^{-1} and temperatures of 250, 350, and 450°C. As on the sample 1.5Cu–ZSM-5–30–0.44, the maximum rate of NO decomposition on the catalysts with Cu/Al > 0.35 was reached at temperatures of 350–400°C. In this case, the catalytic activity of Cu–ZSM-5 dramatically increased as the Cu/Al ratio was increased from 0.25 to 0.35–0.40, and a tendency toward a decrease in the activity was subsequently observed. This tendency weakened as the temperature was increased from 250 to 450°C, and the rate of NO decomposition on the catalysts with Cu/Al from 0.5 to 1.1 at 450°C remained almost unchanged. The dependences shown in Fig. 6 are consistent with published data [7, 20, 31, 36–38]. For example, it was shown that the Cu–ZSM-5 catalysts with Cu/Al < 0.20 did not exhibit activity in the reaction of NO decomposition [7]; however, their efficiency increased as the Cu/Al ratio was increased from 0.20 to 0.45 [7, 34] and reached a maximum value at Cu/Al close to 0.50–0.60 [1, 7]. These data were confirmed by the results of studies [36, 38] performed on Cu–ZSM-5 catalysts with Si/Al = 12–25. A number of authors showed that the over-exchanged Cu–ZSM-5 catalysts were active and stable in the reaction of NO decomposition. In this case, the same conversion of NO was reached on the samples with Cu/Al = 0.65–0.75 [36–39] and the activity remained unchanged [1, 37–39] or gradually decreased [7] as this ratio was further increased to 0.75–0.90. On the other hand, the rate of NO decomposition on Cu–ZSM-5 with a high modulus (Si/Al = 80) increased as Cu/Al was increased up to 2.87 [40] and 3.20 [21].

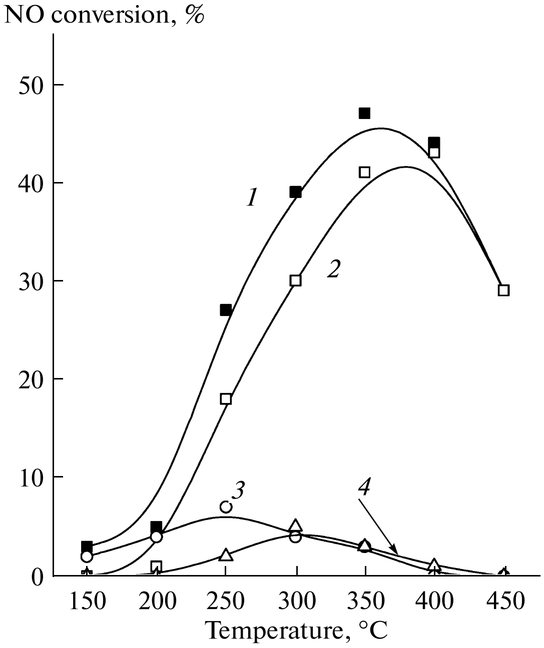

Fig. 5. The temperature dependence of the NO conversion on the catalyst 1.5Cu–ZSM-5–30–0.44 at a space velocity of 5200 h^{-1} and an NO concentration of 1.5 vol % in helium: (*1*) total conversion, (*2*) conversion into N_2, (*3*) conversion into N_2O, and (*4*) conversion into NO_2.

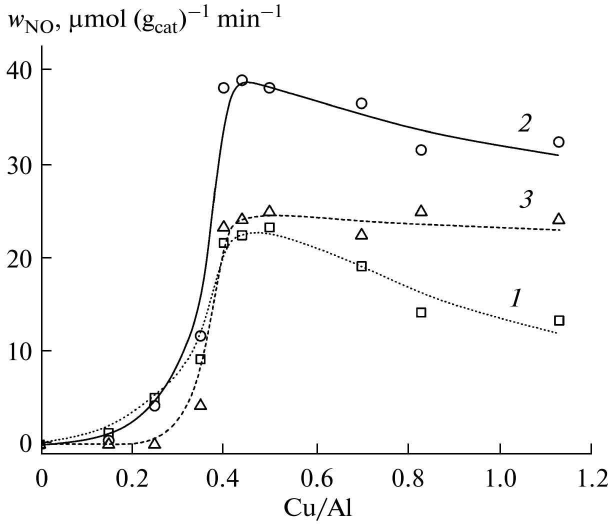

Fig. 6. Dependence of the rate of NO conversion on the catalysts Cu–ZSM-5–30 upon the Cu/Al ratio at (*1*) 250, (*2*) 350, and (*3*) 450°C.

The observed dependence of the catalytic activity of Cu–ZSM-5 in NO decomposition on the Cu/Al ratio (Fig. 6) correlates well with the amount of NO chemisorbed on them (Fig. 4). It was noted above that the amount of NO chemisorbed under the same conditions (initial NO pressure of 2.6 mbar and temperature of 25°C) depends on the Cu/Al ratio in Cu–ZSM-5. The amount of chemisorbed NO increases with an increasing Cu/Al ratio and reaches a maximum (70–80 μmol NO/g_{cat}) at Cu/Al = 0.35–0.40 regardless of the Si/Al ratio and the pH of a copper acetate solution used in the synthesis of Cu–ZSM-5. At the above Cu/Al ratios, a maximum rate of NO decomposition, in particular, with the formation of N_2O, was reached (Fig. 6). The intensities of the absorption bands at 18400 and 25600 cm^{-1} in the UV-Vis DR spectrum increased symbatically. As noted above, these absorption bands are due to the formation of NO complexes with Cu^+ and Cu^{2+} cations, which are the constituents of copper oxide structures containing two or more copper ions. The amount of NO chemisorbed at 25°C remained unchanged up to a Cu/Al ratio close to 0.50; however, with a further increase in the Cu/Al ratio to 0.65–0.85, a tendency toward a certain decrease in the chemisorption of NO was observed (55–60 μmol NO/g_{cat}). Analogously, a tendency toward a decrease in the activity of over-exchanged catalysts took place; this tendency was most clearly pronounced at low temperatures (250°C, Fig. 6).

On the other hand, the low-temperature adsorption of NO on Cu–ZSM-5 has some specific features, as compared with its activity in NO decomposition at elevated temperatures. The maximum ratio of the amount of chemisorbed NO to the total copper content (NO/Cu) was 0.27–0.30, and it was observed in the Cu–ZSM-5 samples in the wide range of Cu/Al ratios from 0.25 to 0.45. Thus, even in the samples with Cu/Al = 0.25–0.45, no more than 30% copper introduced into Cu–ZSM-5 is capable of actively adsorbing NO at 25°C, and the fraction of this active copper decreased in both over-exchanged samples (NO/Cu = 0.15 at Cu/Al > 0.5) and samples with a low exchange level (NO/Cu < 0.1 at Cu/Al < 0.15). At the same time, the Cu–ZSM-5 samples with Cu/Al in the narrow range from 0.37 to 0.45 exhibited the maximum catalytic activity per gram of copper at temperatures of 250–450°C, and the activity decreased as the Cu/Al ratio was increased and, particularly sharply, as this ratio was decreased.

The above specific features of the catalytic behavior of Cu–ZSM-5 in NO decomposition are adequately described by the proposed reaction scheme of NO conversion. The high catalytic activity of the Cu–ZSM-5 samples with Cu/Al of about 0.4 can be explained by the formation of a sufficient amount of chain copper oxide structures in zeolite channels; these structures contained at least two closely spaced copper ions connected by extra-framework oxygen. The activation of NO molecules occurs with the participation of Cu^+ ions, which are the constituents of these structures. This activation occurs through the formation of the π-radical anion of the *cis* dimer of N_2O_2 and new active centers, in particular, $[Cu^{2+}O^-]$, which subsequently participate in the decomposition of NO at elevated temperatures. The experimentally found formation of N_2O and NO_2 products at temperatures lower than 350°C can be explained by the destruction of the complexes $[Cu^{2+}\text{–}cis\text{-}(N_2O_2)^-]$ and $[Cu^{2+}(NO_3)^-]$, respectively. According to published data [34], the dimers $[Cu\text{–}O\text{–}Cu]^{2+}$ are active in the reaction of NO decomposition; it was assumed that these dimers are formed in over-exchanged catalysts. However, the formation of the dimers of copper and copper oxide structures in the catalysts with Cu/Al < 0.5 cannot also be excluded because of the special features of the hydrolysis of copper salts. For example, with the use of a solution of copper acetate with pH ~6.0 instead of pH 5.74 (Cu/Al = 0.48 and 0.52, respectively) for the synthesis, the conversion of NO on the Cu–ZSM-5 samples with close exchange levels differed by almost 20% [36]. At the same time, the catalysts with Cu/Al = 0.48 and 0.51 obtained at pH 5.74 exhibited the same activity. In a number of publications [39–42], it was assumed that the high activity of Cu–ZSM-5 catalysts with a low silica modulus (Si/Al = 12 and 26 [40]) and Cu/Al ratios of 0.45–0.75 in the reaction of NO decomposition at 500°C was caused by the formation of an optimum number of active centers containing two closely spaced copper atoms [1, 39], in particular, in the microcrystallites of Cu_xO_y on the catalyst surface [42].

It is likely that isolated Cu^{2+} ions can participate in the adsorption of NO. This is evident from the chemisorption of NO in an amount to 20–30 μmol/g_{cat}, which is characteristic of the Cu–ZSM-5 catalysts with Cu/Al < 0.20. Furthermore, it is well known that isolated ions with a square-planar ligand environment easily coordinate NO [43], and the IR spectra exhibit signals due to $Cu^+NO^{\delta-}$, $Cu^+(NO)_2^{\delta-}$, and $Cu^{2+}(NO)^{\delta+}$ [34, 44, 45]. However, it is likely that the chemical adsorption of NO on isolated Cu^{2+} ions is not accompanied by the low-temperature activation of NO [34] because, according to our results and published data [7, 20, 34], the Cu–ZSM-5 catalysts with Cu/Al < 0.2 do almost not manifest catalytic activity in the decomposition of NO at temperatures of 250–450°C.

The influence of oxygen on the activity of Cu–ZSM-5 in the reaction of NO decomposition, which depends on the copper content of the catalyst [7, 20], can be adequately explained by the participation of the same centers, namely, the Cu^+ ions of chain structures, in the adsorption of oxygen and the activation of NO. The introduction of oxygen into a gas mixture decreased the rate of NO decomposition, but the conversion of NO increased with the copper content of the catalyst even under these conditions [7, 20, 41]. For example, oxygen had a weak effect on the activity of Cu–ZSM-5 with Cu/Al of ≈ 0.6, whereas the catalyst with Cu/Al of ≈ 0.45 was strongly deactivated in this case [7].

Thus, the oxidation–reduction properties of chain copper oxide structures in zeolite channels, namely, their capability for the reversible reduction of the Cu^{2+}

ions to Cu^+ and the oxidation of the Cu^+ ions to Cu^{2+}, and the stabilization of the mixed-valence bound states $Cu^{2+}\ldots Cu^+$ under mild reduction conditions impart unique catalytic characteristics to Cu–ZSM-5 for the reactions of direct NO decomposition.

ACKNOWLEDGMENTS

This work was supported by the Presidium of the Russian Academy of Sciences (program "Basic Research in Nanotechnologies and Nanomaterials," project no. 21-41) and the Russian Foundation for Basic Research (grant no. 08-03-90435).

REFERENCES

1. Iwamoto, M., Yahiro, H., Mine, Y., and Kagawa, S., *Chem. Lett.*, 1989, no. 2, p. 213.
2. Kharas, K.C.C., Liu, D.-J., and Robota, H.J., *Catal. Today*, 1995, vol. 26, p. 129.
3. Smeets, P.J., Groothaert, M.H., Teeffelen, R.M., Leeman, H., Hensen, E.J.M., and Schoonheydt, R.A., *J. Catal.*, 2007, vol. 245, p. 358.
4. Held, W., Konig, A., Richter, T., and Puppe, L., *SAE Tech. Paper Series*, 1990, paper 900496, p. 13.
5. Iwamoto, M. and Hamada, H., *Catal. Today*, 1991, vol. 10, p. 57.
6. Petunchi, J.O., Sill, G., and Hall, W.K., *Appl. Catal., B*, 1993, vol. 2, p. 303.
7. Iwamoto, M., Yahiro, H., Tanda, K., Mizuno, N., Mine, Y., and Kagawa, S., *J. Phys. Chem.*, 1991, vol. 95, p. 3727.
8. Yashnik, S.A., Ismagilov, Z.R., and Anufrienko, V.F., *Catal. Today*, 2005, vol. 110, p. 310.
9. Groothaert, M.H., van Bokhoven, J.A., Battiston, A.A., Weckhuysen, B.M., and Schoonheydt, R.A., *J. Am. Chem. Soc.*, 2003, vol. 125, p. 7629.
10. Kuroda, Y., Kotani, A., Maeda, H., Moriwaki, H., and Morimato, T., *J. Chem. Soc., Faraday Trans.*, 1992, vol. 88, p. 1583.
11. Shapiro, E.S., Gruner, W., Joyner, R.W., and Baeva, G.N., *Catal. Lett.*, 1994, vol. 24, p. 159.
12. Ismagilov, Z.R., Yashnik, S.A., Anufrienko, V.F., Larina, T.V., Vasenin, N.T., Bulgakov, N.N., Vosel, S.V., and Tsykoza, L.T., *Appl. Surf. Sci.*, 2004, vol. 226, nos. 1–3, p. 88.
13. Krivoruchko, O.P., Anufrienko, V.F., Paukshtis, E.A., Larina, T.V., Burgina, E.B., Yashnik, S.A., Ismagilov, Z.R., and Parmon, V.N., *Dokl. Phys. Chem.*, 2004, vol. 398, no. 1, p. 226.
14. Lever, A.B.P., *Inorganic Electronic Spectroscopy*, New York: Elsevier, 1984.
15. Yan, J.Y., Lei, G.-D., Sachtler, W.M.H., and Kung, H.H., *J. Catal.*, 1996, vol. 161, p. 43.
16. Montreuil, C.N. and Shelef, M., *Appl. Catal., B*, 1992, vol. 1, p. L1.
17. Yashnik, S.A., Anufrienko, V.F., Zaikovskii, V.I., Rogov, V.A., Ruzankin, S.Ph., and Ismagilov, Z.R., *Stud. Surf. Sci. Catal.*, 2008, vol. 174A, p. 177.
18. Anufrienko, V.F., Yashnik, S.A., Bulgakov, N.N., Larina, T.V., Vasenin, N.T., and Ismagilov, Z.R., *Dokl. Phys. Chem.*, 2003, vol. 392, nos. 1–3, p. 207.
19. Zakharov, I.I., Ismagilov, Z.R., Ruzankin, S.Ph., Anufrienko, V.F., Yashnik, S.A., and Zakharova, O.I., *J. Phys. Chem. C*, 2007, vol. 111, p. 3080.
20. Iwamoto, M. and Yahiro, H., *Catal. Today*, 1994, vol. 22, p. 5.
21. Pirone, R., Ciambelli, P., Moretti, G., and Russo, G., *Appl. Catal., B*, 1996, vol. 8, p. 197.
22. Mason, J., *J. Chem. Soc., Dalton Trans.*, 1974, p. 19.
23. Pulidoa, A. and Nachtigall, P., *Phys. Chem. Chem. Phys.*, 2009, vol. 11, p. 1447.
24. McKellar, A.R.W., Watson, J.K.G., and Howard, B., *J. Mol. Phys.*, 1995, vol. 86, p. 273.
25. Snis, A. and Panas, I., *Chem. Phys.*, 1997, vol. 221, p. 1.
26. Valentin, C., Pacchioni, G., Abbet, S., and Heiz, U., *J. Phys. Chem. B*, 2002, vol. 106, p. Ð. 7666.
27. Kutepov, A.M, Bondareva, T.I., and Berengarten, M.G., *Obshchaya khimicheskaya tekhnologiya* (General Chemical Technology), Moscow: Vysshaya Shkola, 1990.
28. Valyon, J. and Hall, W.K., *J. Phys. Chem.*, 1993, vol. 97, p. 1204.
29. Aylor, A.W., Larsen, S.C., Reimer, J.A., and Bell, A.T., *J. Catal.*, 1995, vol. 157, p. 592.
30. Hadjiivanov, K., Klissurski, D., Ramis, G., and Busca, G., *Appl. Catal., B*, 1996, vol. 7, p. 251.
31. Carvalho, M.C.N.A., Passos, F.B., and Schmal, M., *Appl. Catal., A*, 2000, vol. 193, p. 265.
32. Li, Y. and Armor, J.N., *Appl. Catal.*, 1991, vol. 76, p. L1.
33. Spoto, G., Zecchina, A., Bordiga, S., Ricchiardi, G., Martra, G., Leofanti, G., and Petrini, G., *Appl. Catal., B*, 1994, vol. 3, p. 151.
34. Iwamoto, M., Yahiro, H., Mizumo, N., Zhang, W.-X., Mine, Y., Furukawa, H., and Kagawa, S., *J. Phys. Chem.*, 1992, vol. 96, p. 9360.
35. Kapteijn, F., Marban, G., Rodriguez-Mirasol, J., and Moulijn, J.A., *J. Catal.*, 1997, vol. 167, p. 256.
36. Zhang, Y., Leo, K.M., Sarofim, A.F., Hu, Z., and Flytzani-Stephanopoulos, M., *Catal. Lett.*, 1995, vol. 31, p. 75.
37. Yokomichi, Y., Yamabe, T., Kakumoto, T., Okada, O., Ishikawa, H., Nakamura, Y., Kimura, H., and Yasuda, I., *Appl. Catal., B*, 2000, vol. 28, p. 1.
38. Campa, M.C., Indovina, V., Minelli, G., Moretti, G., Pettiti, I., Porta, P., and Riccio, A., *Catal. Lett.*, 1994, vol. 23, p. 141.
39. Moretti, G., *Catal. Lett.*, 1994, vol. 28, p. 143.
40. Moretti, G., Dossi, C., Fusi, A., Recchia, S., and Psaro, R., *Appl. Catal., B*, 1999, vol. 20, p. 67.
41. Li, Y. and Hall, W.K., *J. Phys. Chem.*, 1990, vol. 94, no. 16, p. 6145.
42. Hamada, H., Kintaichi, Y., Sasaki, M., and Ito, T., *Appl. Catal., A*, 1990, vol. 64.
43. Kucherov, A.V., Gerlock, G.L., Jen, H.-W., and Shelef, M., *Catal. Today*, 1996, vol. 27, p. 79.
44. Dedecek, J. and Wichterlova, B., *J. Phys. Chem. B*, 1997, vol. 101, p. 10233.
45. Wichterlova, B., Sobalik, Z., and Dedecek, J., *Catal. Today*, 1997, vol. 38, p. 199.